

## Effect of parapets to pressure distribution on flat top of a finite cylinder

Y. Ozmen\*

*Department of Mechanical Engineering, Karadeniz Technical University, Trabzon 61080, Turkey*

*(Received August 14, 2012, Revised May 6, 2013, Accepted July 2, 2013)*

**Abstract.** In this paper, the effects of parapets on the mean and fluctuating wind pressures which are acting on a flat top of a finite cylinder vertically placed on a flat plate have experimentally been investigated. The aspect ratio (AR) of cylinder is 1 and the Reynolds number (Re) based on cylinder diameter and free stream velocity is 150000. The pressure distributions on the flat top and the side wall of the finite cylinder immersed in a simulated atmospheric boundary layer have been obtained for different parapet heights. The large magnitudes of mean and minimum suction pressures occurring near the leading edge were measured for the cases with and without parapet. They shift to the further downstream on the circular top with increasing parapet height. It is seen that the parapets reduce the local high suction on the top up to 24%.

**Keywords:** parapet; suction pressure; flat top; finite cylinder; wind tunnel

---

### 1. Introduction

Finite cylindrical structures have been widely used in many engineering applications such as tall buildings, chimney stacks, nuclear cooling towers, offshore structures and cylindrical tanks because of attractive architectural shapes. Many high-rise buildings can be simplified to a finite cylinder with a free end. The study of finite-span bluff bodies located in an atmospheric boundary layer is of interest due to its practical importance in civil and wind engineering applications (Uematsu *et al.* 1990, Fox *et al.* 1993). The flow around the finite cylinder is sufficiently complex that further study is needed to better understand the flow field. The presence of a free end modifies the flow structure in the near-wake region such as turbulent structure and surface pressure distribution. For this reason, the evaluation and improvement of the pressure distribution on the flat tops is very important for civil and wind engineering. Studies related to the understanding of flow field around finite cylinders have aimed the determination of wake structure behind the cylinder and the surface pressure distribution.

Purdy *et al.* (1967) obtained pressure distributions on the cylinders with a flat top. Okomato and Yagita (1973) conducted surface pressure measurements on cylinders with aspect ratios between 1 and 12.5 and found that the drag coefficient decreased with decreasing aspect ratio.

---

\*Corresponding author, Assistant Professor, E-mail: [yozen@ktu.edu.tr](mailto:yozen@ktu.edu.tr)

Farivar (1981) investigated the effect of finite cylinder free end on the mean pressure, pressure fluctuations and drag force. Kawamura *et al.* (1984) tested cylinders with various aspect ratios performing flow visualization, hot-wire measurements and pressure measurements.

They reported the existence of a pair of trailing vortices formed at the free end of the cylinder. Sun *et al.* (1992) investigated the pressure fluctuations on two circular cylinders at high Reynolds number for various arrangements of the cylinders with respect to the flow. Okamoto and Sunabashiri (1992) found that the wake behind the finite cylinder of small aspect ratio is symmetric. Shih *et al.* (1993) reported the results of an experimental study of flow passing rough circular cylinders at large Reynolds number utilizing a pressurized wind tunnel. Kareem and Cheng (1999) experimentally obtained mean and fluctuating pressure distributions on a cylinder of finite height in simulated turbulent boundary layer flows at subcritical Reynolds numbers. Kitagawa *et al.* (2002) measured wind pressure acting on a rigid circular tower and studied the characteristics of the pressures originated tip-associated vortices. Park and Lee (2002) investigated the wake structure behind an isolated finite cylinder embedded in various atmospheric boundary layers with the measurements of wake velocity and mean pressure distribution on the cylinder surfaces. Park and Lee (2003) examined the effect of the gap distance between two finite cylinders embedded in atmospheric boundary layer on the flow characteristics of the near-wake and elucidated the flow structure near the finite cylinder free end in detail. Pattenden *et al.* (2005) studied the flow over a finite-height cylinder of aspect ratio 1 by means of surface flow visualization, particle image velocimetry and surface pressure measurements. Dobriloff and Nitshe (2009) conducted the surface pressure and wall shear stress measurements on a finite wall mounted circular cylinder and in the vicinity of cylinder.

Uematsu *et al.* (1999) presented the results of a wind pressure measurement in a wind tunnel as well as a dynamic-response analysis of a flat top. The results indicated that the gust loading factor approach can be applied to the evaluation of the design wind loads for the structural frame of flat tops. Li *et al.* (2006) obtained wind pressure distributions on cylindrical shells considering different aspect ratios in the wind tunnel models. Sumner and Heseltine (2008) experimentally studied the wake of a finite circular cylinder mounted normal to a ground plane in a low-speed wind tunnel. Uematsu *et al.* (2008) investigated the characteristics of wind pressures acting on flat tops with a wind tunnel experiment. Hain *et al.* (2008) performed tomographic and time resolved PIV measurements to examine the 3D flow topology and the flow dynamic above the upper surface of a low-aspect ratio cylinder. Uematsu and Yamada (1994) experimentally investigated aerodynamic forces on a cantilevered circular cylinder in a wind tunnel using rough-walled models.

Their results indicate that the aerodynamic coefficients are primarily functions of the aspect ratio and the surface roughness of the cylinder. Roh and Park (2003) studied the vertical flow patterns over the free end surface of a finite circular cylinder through the oil streak line method at moderately high Reynolds number. The results of the oil flow visualization show that the flow over the free end is characterized by the separation from the sharp leading edge. A complex three-dimensional recirculation region is formed on top of the cylinder. Two foci and two saddle points are observed on the free-end. Uematsu and Yamada (2002) presented a simplified model for evaluating the design wind loads for structural frames of flat tops.

Fröhlich and Rodi (2004) investigated flow field around a surface mounted circular cylinder of height 2.5 times the diameter by using large eddy simulation method. They showed that the results obtained from numerical model are in fairly good agreement with measurements. Afgan *et al.* (2007) numerically investigated flow structure around wall mounted circular cylinders of finite

height for different aspect ratios with large eddy simulation (LES) and then compared with experimental results. They found that pressure coefficient profile at mid-height of finite cylinder is significantly different from that of an infinite cylinder. Krajnovic (2011) was investigated the flow around a tall fine cylinder using LES. The flow resulting from the LES was used to present a detailed picture of both the instantaneous and the time-averaged flow.

There is little information available in the literature about the parapet effects to the wind loads on the flat tops of finite cylinders. Most of the studies about the parapet effects on the surface pressure distributions are on the low-rise rectangular buildings with flat roof. An experimental study for the evaluation of wind loads on the low-rise building roofs with parapets has been conducted by Stathopoulos (1982). Stathopoulos and Baskaran (1988) experimentally investigated the parapet effects on the flat roofs and they reported that parapets have decreased the suction effects on the roof edges and corners but have increased on the interior part of the roof surface.

Kareem and Lu (1992) determined the mean and fluctuating pressure distributions on a flat roof by using different parapet configurations. They noticed that the parapets have affected the mean and the peak pressure distributions on the roof. Kopp *et al.* (2005) examined the effects of the parapets on the wind-induced loads on the roof corners of low-rise buildings with pressure measurements. They found that the parapets alter the suction loads on the roof by changing the location of the corner vortex relative to the roof. Mans *et al.* (2005) carried out a set of pressure measurements on parapet surfaces to analyze the effect of parapets on wind-induced loads on low-rise buildings. They noted that the worst structural load coefficients over all wind angles are approximately constant with the same ratio of the parapet and building heights because of opposing trends of the pressures on the interior and exterior parapet surfaces.

Parapets are very effective in reducing the magnitude of local suctions near the leading edge at the flat roofs. This feature is related to the fact that parapets lift up the separated shear layer in normal winds. The effects of parapets on the pressure distribution depend on different parameters, such as building geometry and the parapet height. The determination of wind induced loads on the flat tops of cylindrical buildings is necessary for the design of the flat roofs and the knowledge of the effects of architectural details on these loads is also of interest. It is also important to define both the location and magnitude of these suctions. The effect of parapet on the wind loads acting on a finite cylinder have to be analyzed also from the economical side for the reduction of wind loads. The purpose of this study is to examine the distributions of wind loads on flat tops of finite cylinders and to determine the appropriate height of parapet used for reducing the critical suction loads.

## 2. Experimental details

The experiments were carried out in a low speed, open circuit wind tunnel with a test section of 457 mm high, 457 mm wide and 2450 mm long. The combination of barrier, vortex generators and roughness elements at the entrance to the test section was used to simulate atmospheric boundary layer (power-law exponent,  $n=0.2$ ) over a city suburb. Cylindrical model was constructed to a geometric scale of 1:50. A turbulent boundary layer of 150 mm thickness was obtained at the free stream velocity of 15 m/s, giving a Reynolds number based on cylinder diameter of  $Re=150000$ . Fig. 1 indicates a schematic diagram of the wind tunnel test-section and the measurement system.  $\delta$  and  $H$  represent the boundary layer thickness and characteristic height of model, respectively.

The ratio of boundary layer thickness to model height ( $\delta/H$ ) is 1. The mean and fluctuating

surface pressure measurements were conducted with a measurement chain system consisting of the components of signal conditional module, Setra 239 pressure transducer, A/D converter, package and computer. The output of the pressure transducer was fed through a signal conditioning unit before being digitized and recorded. The signals from the transducer are sampled at a rate of 1000 samples per second for a period of 16 s and data were low-pass filtered at 300 Hz. Measurements have been performed at the spacing of  $15^\circ$  wind angle along the mid-axis of the model. The mean and fluctuating velocity measurements at the reference boundary layer were performed with TSI IFA 100 constant-temperature anemometer and TSI model 1211 hot-film probe.

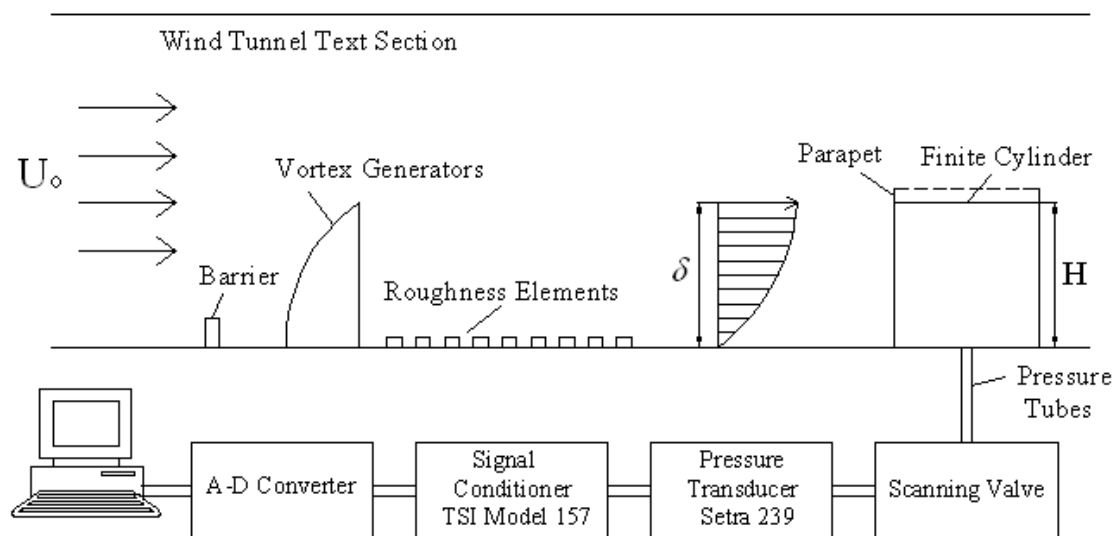


Fig. 1 Wind tunnel test section and pressure measurement system

The cylindrical models and the distribution of the measurement taps on their surfaces are shown in Fig. 2. The finite cylinder models used in this study were made of polyvinyl chloride. The dimensions of models used in the experiments were  $H=150$  mm,  $D=150$  mm (aspect ratio of 1).  $H$  represent model height and  $D$  is the model diameter. Parapets having 1 mm thickness and different heights are placed to the edge of the top. The pressures on the top and wall of model were measured for non-parapet configuration ( $h=0$  mm) and three different parapet heights of  $h=5$ , 10 and 15 mm. To measure the surface pressure distributions, 16 pressure taps in inner diameter of 0.8 mm were placed on the top and the side wall of cylinder and the model was rotated from  $0^\circ$  to  $180^\circ$  in  $15^\circ$  increments in a counter clockwise direction ( $\theta$ ) as incoming flow. A scanning valve was used to supply linkage from pressure taps to pressure transducer. All pressure taps were connected to the scanning valve using the vinyl tubing of 60 cm lengths and 1 mm inside diameter. The pressure difference between the local surface pressure ( $P$ ) and the static pressure ( $P_0$ ) was divided by the reference dynamic pressure at a equivalent height to give pressure coefficient  $C_p$  expressed as  $C_p=(P-P_0)/0.5\rho U_0^2$ , where  $U_0$  is the free-stream velocity and  $\rho$  is the air density. Ambient temperature and atmospheric pressure were continuously recorded during the experiments

to identify changes in the air density. The blockage ratio defined as the ratio of the projected cylinder area to the cross-sectional area of test section is about 10%. Correction for the effect of the wind tunnel blockage was made in this study. West and Apelt (1982) found that the surface pressure distribution on the finite circular cylinder varies only slightly with respect to the blockage ratio of the model. The uncertainties of mean and fluctuating velocity measurements are found as  $\pm 2\%$  and  $\pm 4\%$ , respectively. The uncertainties of mean and fluctuating pressure measurements are  $\pm 3\%$  and  $\pm 4.5\%$ , respectively (Holman, 1994). The uncertainty of the mean drag coefficient,  $C_D$ , was estimated at  $\pm 2\%$ . The experimental results were reproducible within these uncertainty ranges.

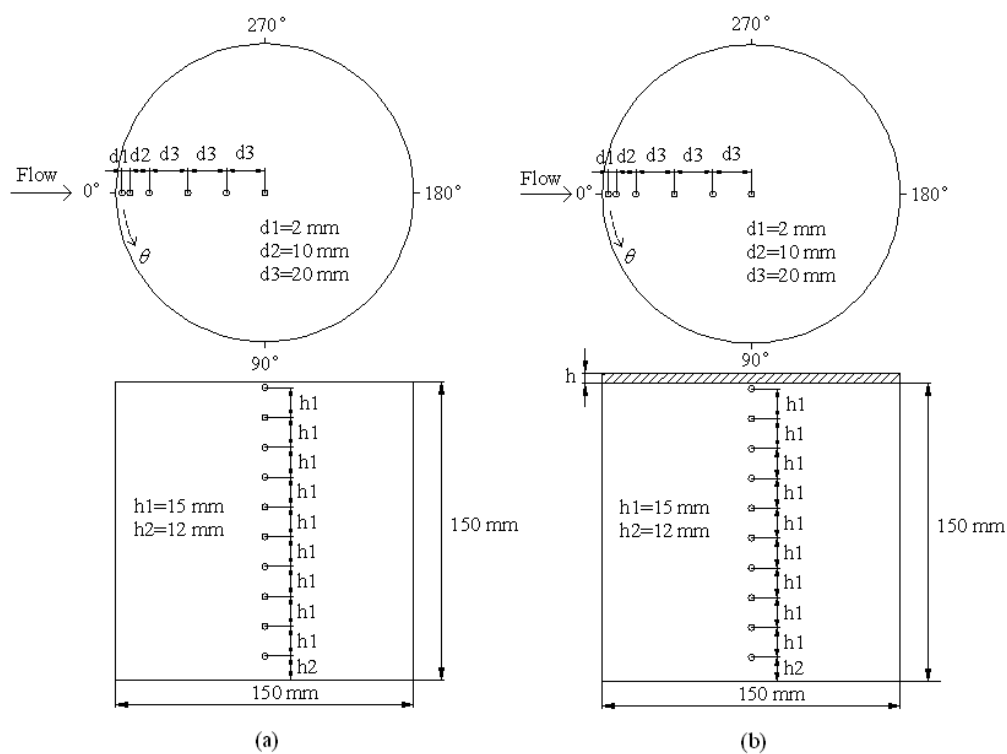


Fig. 2 The dimensions of cylinder having to flat top (a) non-parapet (b) with parapets of  $h = 5, 10, 15$  mm

### 3. Result and discussion

The mean velocity and turbulence intensity profiles of the stream wise velocity components measured at the reference boundary layer are shown in Fig. 3. It is seen that the mean velocity profile in the reference boundary layer agrees well with the power law of  $n=0.2$  and the turbulence intensity near the wall reaches up to 11%.

The resulting data consists of mean, maximum, minimum and root-mean-square (rms) values of the surface pressure which have been normalized by the free stream mean dynamic pressure. The variations of mean, maximum, minimum and rms values of pressure coefficients along the mid-axis of finite cylinder model are given comparatively with measurements of Uematsu *et al.*

(2008) in Fig. 4. Pressure distribution on the windward wall is positive due to impinging effect. Negative pressure fields occur both on the top and side walls of cylinders because of flow separating from the leading edge of the top. The flow separating from the leading edge of flat top reattaches downstream on the top. The largest negative pressures occur in the separation flow region near the leading edge of the top and are progressively reduced in magnitude in the reattachment region on the top surface. Pressure distribution along the leeward wall is almost uniform and is under the atmospheric pressure. It is seen from the figure that there is a good accordance between the mean pressure distributions of present study and Uematsu *et al.* (2008) measurements.

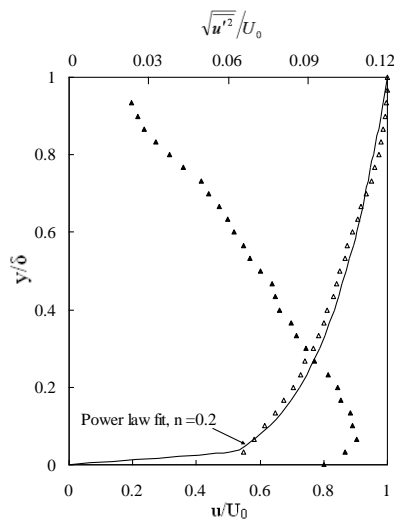


Fig. 3 Profiles of mean velocity and turbulence intensity

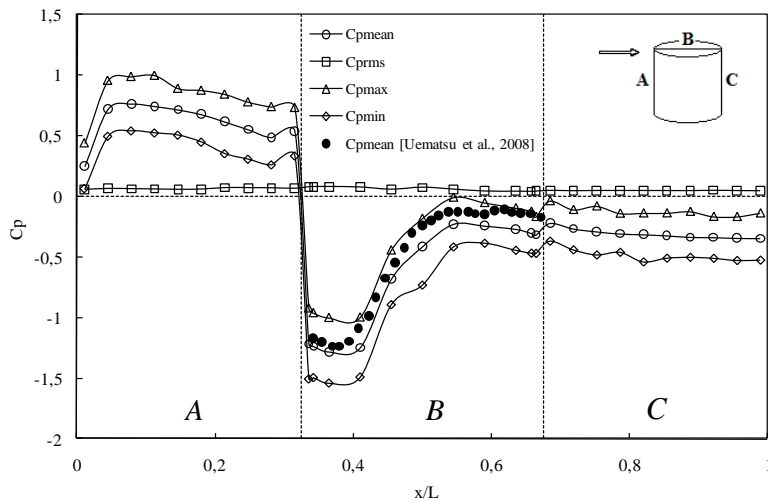


Fig. 4 Variation of pressure coefficients along the mid-axis of cylindrical model with flat top in the flow direction

Figs. 5 and 6 show the mean and minimum pressure distributions on the flat top without parapet and cylinder surface. Fig. 5(a) shows the contours with mean pressure coefficients obtained for the flat top of the finite cylinder. There is a symmetrical behavior for the pressures measured on the top with respect to the windward meridian. The contour lines are roughly perpendicular to the wind direction, except the leeward edge of the top where a three-dimensional effect becomes significant. Only the negative values were observed on the top, which represents suction or pressures exerted in an outward direction. Critical negative pressures were obtained on the windward part of the top. At this region, high negative values are expected due to separation of flow induced by the sudden change in the meridian between the cylinder wall and the top surface.

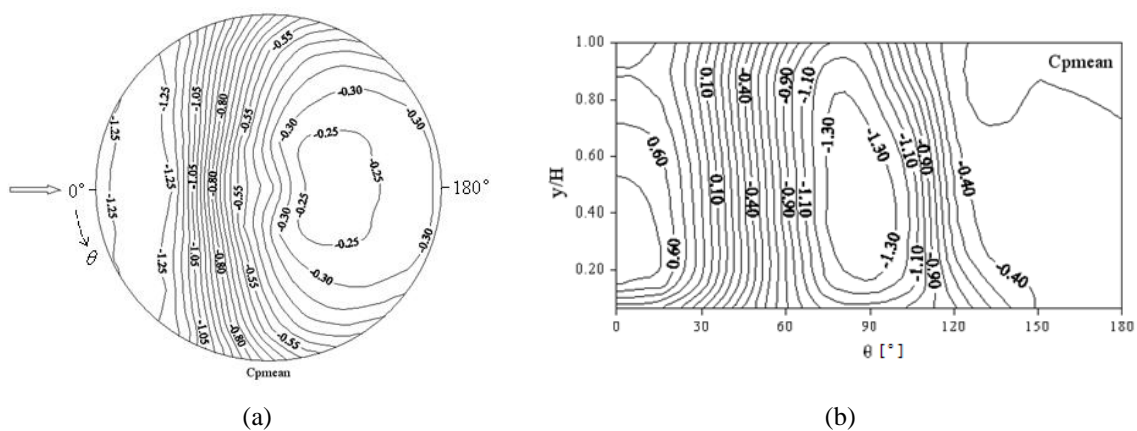


Fig. 5 Contour of mean pressure coefficients in the cylindrical model with a flat top (a) top and (b) cylinder

Portela and Godoy (2005) also found the values similar to those of the present study on the windward region of the top. The highest suction was measured on the windward region of the top with  $C_{p_{\text{mean}}} = -1.25$ , as an approximate value of  $C_{p_{\text{mean}}} = -0.25$  was obtained at the leeward region of the top. Contours of mean wind pressure coefficients were plotted along the circumference of the cylinder and are shown in Fig. 5(b). The positive pressure coefficients were obtained on the windward meridian, while the critical negative suction were found at an angle close to  $90^\circ$  from windward. Due to the accelerating flow around the finite cylinder, the mean pressure coefficients decreases from 0.60 to -1.30 for cylinder angles of  $\theta = 0^\circ$  and  $90^\circ$  and the flow separates from the cylinder surface around  $\theta = 90^\circ$ . The critical values were measured between 20% and 80% of the height of the model. The pressure coefficients measured at the leeward meridian on the top of the cylinder are similar to those measured in the leeward region of the top. The cylinder top is characterized by two symmetrical regions of minimum pressure coefficients on the windward part of the top corresponding to two vortex centers constraining a separation bubble on the top and by a reattachment region on the leeward part of the top as shown in Fig. 6(a). The pressures increase with minimum pressure coefficients of  $C_{p_{\text{min}}} = -1.55$  to -0.40 on the flat top from the windward region to leeward region. Critical minimum suction measured on the flat top and cylinder surface are 25% higher than the mean pressure coefficients (Figs. 6(a) and 6(b)). Similar findings were also obtained by Roh and Park (2003).

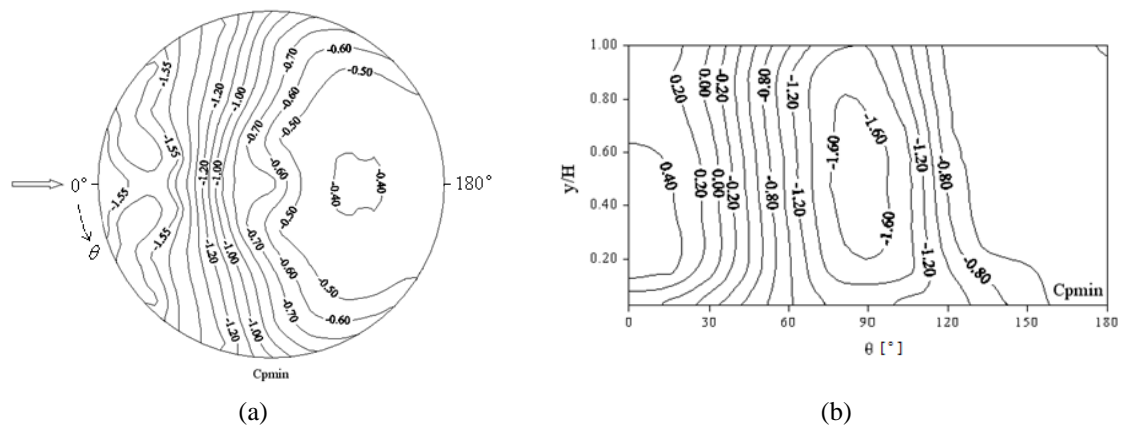


Fig. 6 Contour of minimum pressure coefficients in the cylindrical model with a flat top (a) top and (b) cylinder

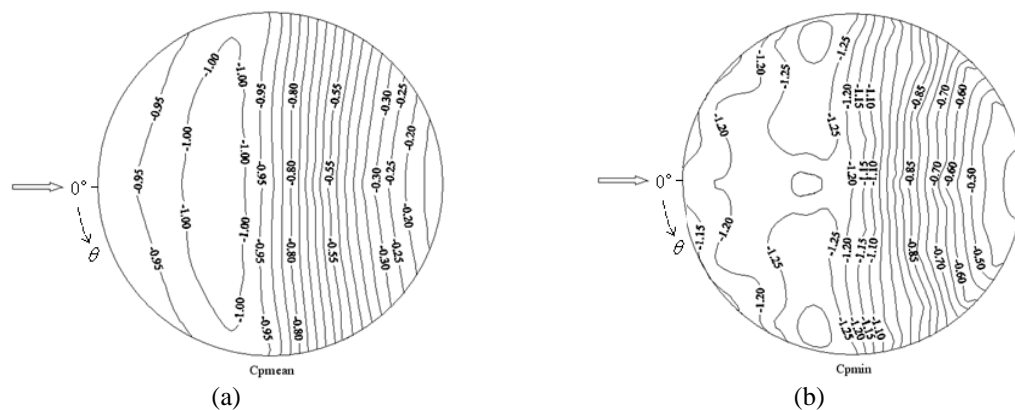


Fig. 7 Contour of pressure coefficients on flat top with the parapet height of 5 mm (a) mean and (b) minimum

Figs. 7, 8 and 9 shows contours of mean and minimum pressure coefficients on the flat top with the parapet heights of 5 mm, 10 mm and 15 mm respectively. The contours obtained for the parapet height of 5 mm are given in Figs. 7(a) and 7(b). The highest suction is found as  $C_{p\text{mean}} = -1$  and  $C_{p\text{min}} = -1.25$  on the top. It is seen that with 5 mm height parapet, the local high suction on the top are reduced by 20%. The general reduction is because of the fact that parapets tend to lift the shear layer or the vortices away from the top surfaces. No reattachment region is observed for the flow separating from the leading edge of cylinder top. Because, the shear layer moves higher from the top surface due to the parapet height. Critical negative pressures are found at where the flow is farthest from the top surface. As the flow gets closer to the top surface through the leeward region, pressure recovery is observed at that region. Also, the pressure increases due to the parapet at the leeward side obstructing the flow. Figs. 8a and b show the contours obtained for the parapet height of 10 mm. The highest suction is determined as  $C_{p\text{mean}} = -0.95$  and  $C_{p\text{min}} = -1.20$  on the top. It is seen that local high suction on the top are reduced by 24% in the presence of parapet with 10 mm height. The contours of mean and minimum pressure coefficients on the flat top with

the parapet height of 15 mm are given in Figs. 9(a) and 9(b). The highest suction is obtained as  $C_{p\text{mean}} = -1$  and  $C_{p\text{min}} = -1.25$  on the top. For 15 mm height parapet, a 20 % decrement on the local high suction is obtained. No reattachment regions are also observed for 10 mm and 15 mm parapet heights.

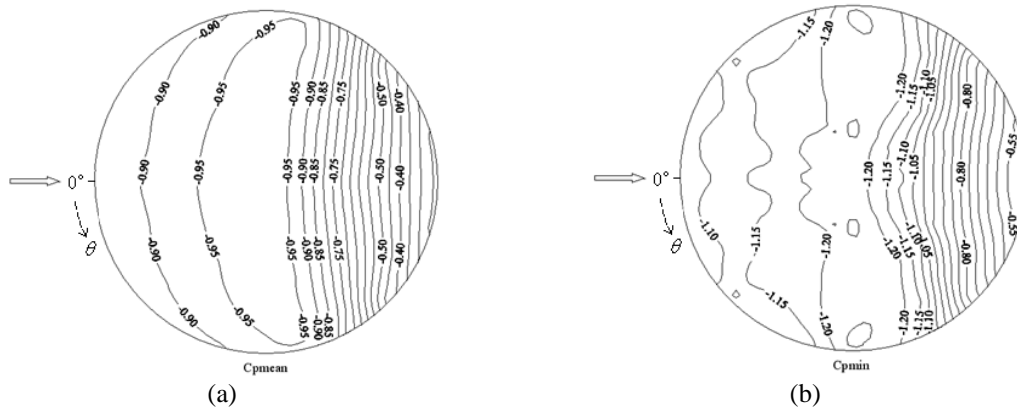


Fig. 8 Contour of pressure coefficients on flat top with the parapet height of 10 mm (a) mean and (b) minimum

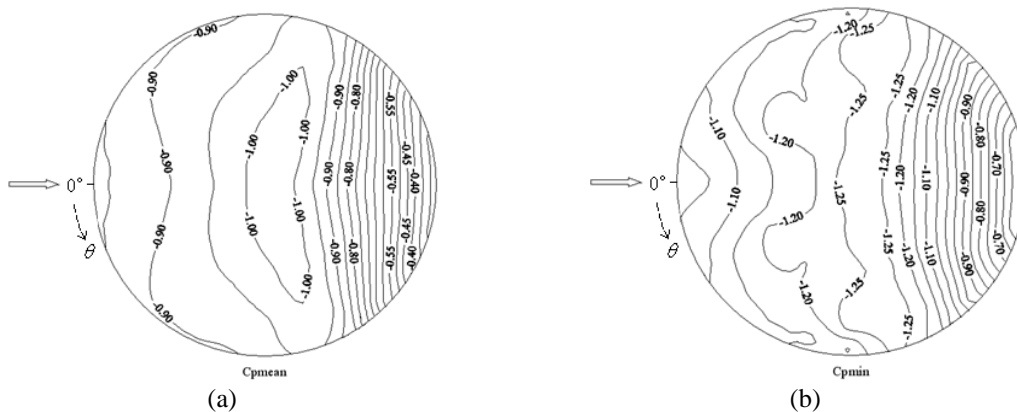


Fig. 9 Contour of pressure coefficients on flat top with the parapet height of 15 mm (a) mean and (b) minimum

The location of the large mean and minimum suction shifts through the downstream on the cylinder top with increasing parapet height. The 10 mm height parapet is found to be the most effective one among the 5 mm, 10 mm and 15 mm ones for relieving the high negative pressure. Critical minimum suction measured on the flat top with three different parapet heights are 25% higher than mean pressure coefficients. The mean and minimum pressures in the interior regions of the tops are slightly affected from the parapets. Although not shown, the pressure patterns on the cylindrical wall for different parapet heights do not present any changes unlike the differences

between pressure distributions found on the top of finite cylinder.

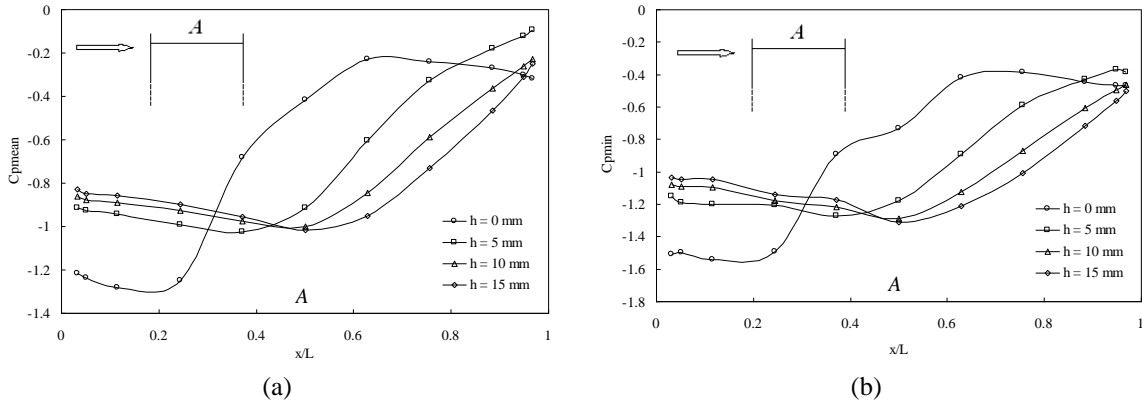


Fig. 10 Comparison of pressure distributions along the mid-axis of flat top for various parapet heights in the flow direction (a) mean and (b) minimum

The variations of mean and minimum pressure coefficients measured along the mid-axis of top for three different parapet heights are presented together with those obtained from non-parapet configuration in Figs.10(a) and 10(b), respectively. It is observed that the parapets are more effective with increasing height for reducing suction pressure coefficients. While there is a reattachment region on the cylinder top without parapet, no reattachment regions are observed on the cylinder top with parapets. The pressure coefficients around the leeward edge of the top are almost the same for all of the investigated parapet heights.

The drag and lift loadings of the finite cylinder with and without parapets are also investigated. The local drag and lift coefficients have been obtained by integrating the pressure distribution over the cylinder surface. The drag coefficient ( $C_D$ ) and the lift coefficient ( $C_L$ ) are calculated by using Eqs. (1) and (2) respectively.

$$C_D = \frac{1}{2} \int_0^{2\pi} C_p \cdot \cos\theta \cdot d\theta \tag{1}$$

$$C_L = -\frac{1}{2} \int_0^{2\pi} C_p \cdot \sin\theta \cdot d\theta \tag{2}$$

Fig. 11 shows the mean pressure distribution and their components along the drag and lift directions around the circumference of the cylinder at different heights above the floor. The drag component of  $C_p$  is  $C_p \cos(\theta)$  and the lift component of  $C_p$  is  $C_p \sin(\theta)$ . The local drag coefficient is calculated in ten different positions along the cylinder wall from the bottom to the top and those ten values are integrated along the cylinder height.  $C_D = 0.52$  is obtained as a mean value for the cylinder without parapet. The same calculation is repeated for the finite cylinder with parapets and the same value is obtained. It is observed that the parapets do not affect the mean drag coefficient. Lift coefficient is also calculated with the same process and  $C_L = 0$  is obtained.

The mean drag coefficient  $C_D$  of several investigations is given in Table 1. It is observed from the table that,  $C_D$  decreases when aspect ratio (AR) reduces due to the intrusion of the flow over the top into the wake.

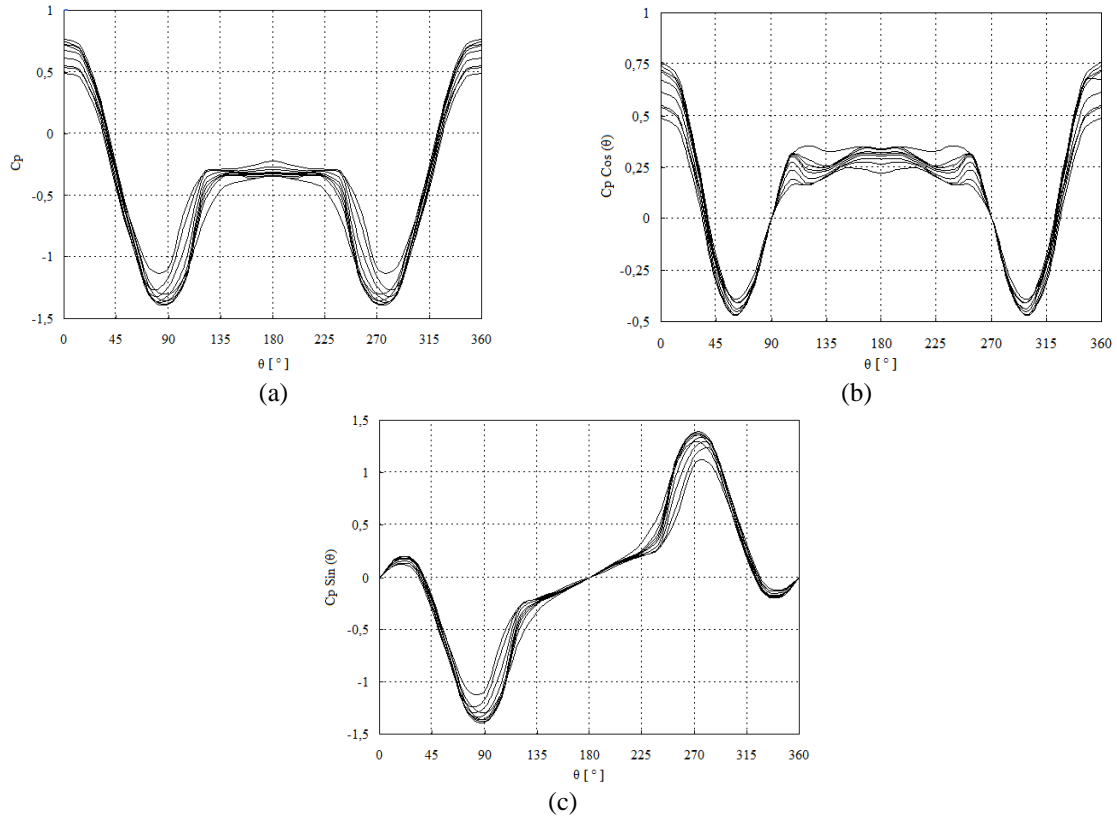


Fig. 11 Mean pressure distributions and their components (a) mean pressure (b) drag component  $C_p \cos\theta$  and (c) lift component  $C_p \sin\theta$

Table 1 Mean drag coefficients compared between various investigations and the present study

Authors	$C_D$	Re	AR
Kawamura <i>et al.</i> (1984)	0.78	$2 \times 10^5$	2
Okamoto <i>et al.</i> (1992)	0.73	$1.3 \times 10^4$	2
Sumner <i>et al.</i> (2004)	0.61	$6 \times 10^4$	3
Sumner <i>et al.</i> (2004)	0.74	$6 \times 10^4$	5
Sumner <i>et al.</i> (2004)	0.78	$6 \times 10^4$	7
Sumner <i>et al.</i> (2004)	0.81	$6 \times 10^4$	9
Frederich <i>et al.</i> (2008)	0.55	$2 \times 10^6$	2
Present study (without parapet)	0.52	$1.5 \times 10^5$	1
Present study (with parapets)	0.52	$1.5 \times 10^5$	1

#### 4. Conclusions

In this study, the influence of parapet height to pressure distribution on the flat top of a finite cylindrical building is experimentally investigated. Mean and minimum pressure distributions due

to wind on the flat top and on the cylindrical wall were obtained for different parapet heights. Negative pressure fields occur on the top and at the leeward wall of the cylinder because of flow separating from the leading edge of the top. The largest negative pressures occur just beyond the separation and are progressively reduced in magnitude in the reattachment region of the top surface. While there is a reattachment region on the cylinder top without parapet, no reattachment regions are observed on the cylinder top with parapets. The magnitude of the peak pressures in the edge region decreases monotonically as the height of the parapet increases. It is seen from the results that the local high suction on the top are reduced up to %24 by the presence of parapets.

This reduction is because of the fact that parapets tend to lift the shear layer away from the top surfaces. The large mean and minimum suction shift through the downstream on the top with increasing parapet height. The mean and minimum pressures in the interior region of the top are little affected by parapets. In all cases the parapet tends to reduce the top pressure. Wall loads remain unaffected by the presence of parapets. The drag and lift coefficients for finite cylinder are found as  $C_D = 0.52$  and  $C_L = 0$ . It can be concluded that the parapets do not affect the mean drag and lift coefficients. It is hoped that this study would serve data for the further researches on this topic.

## References

- Afgan, I., Moulinec, C., Prosser, R. and Laurence, D. (2007), "Large eddy simulation of turbulent flow for wall-mounted cantilever cylinders of aspect ratio 6 and 10", *Int. J. Heat Fluid Fl.*, **28**(4), 561-574.
- Dobriloff, C. and Nitsche, W. (2009), *Surface pressure and wall shear stress measurements on a wall mounted cylinder*, *Imaging Measurement Method.*, NFM **106**.
- Farivar, D. (1981), "Turbulent uniform flow around cylinders of finite length", *AIAA J.*, **19**(3), 275-281.
- Fox, T.A., Apelt, C.J. and West, G.S. (1993), "The aerodynamics disturbance caused by the free-ends of a circular cylinder immersed in a uniform flow", *J. Wind Eng. Ind. Aerod.*, **49**(1-3), 389-400.
- Frederich, O., Wassen, E. and Thiele, F. (2008), "Prediction of the flow around a short wall-mounted finite cylinder using LES and DES", *J. Numer. Anal. Ind. Appl. Math.*, **3**(3-4), 231-247.
- Fröhlich, J. and Rodi, W. (2004), "LES of the flow around a circular cylinder of finite height", *Int. J. Heat Fluid Fl.*, **25**(3), 537-548.
- Hain, R., Köhler, C.J. and Michaelis, D. (2008), "Tomographic and time resolved PIV measurements on a finite cylinder mounted on a flat plate", *Exp. Fluids*, **45**(4), 715-724.
- Holman, J.P. (1994), *Experimental methods for engineers*, McGraw-Hill Book Company, New York.
- Karem, A. and Lu, P.C. (1992), "Pressure fluctuations on flat roofs with parapets", *J. Wind Eng. Ind. Aerod.*, **41-44**, 1775-1786.
- Kareem, A. and Cheng, C.M. (1999), "Pressure and force fluctuations on isolated roughened circular cylinders of finite length in boundary layer flows", *J. Fluid. Struct.*, **13**(7-8), 907-933.
- Kawamura, T., Hiwada, M., Hibino, T., Mabuchi, I. and Kamuda, M. (1984), "Flow around a finite circular cylinder on a flat plate", *Bull. JSME*, **27**(232), 2142-2151.
- Kitagawa, T., Fujino, Y., Kimura, K. and Mizuno, Y. (2002), "Wind pressures measurement on end-cell-induced vibration of a cantilevered circular cylinder", *J. Wind Eng. Ind. Aerod.*, **90**(4-5), 395-405.
- Kopp, G.A., Mans, C. and Surry, D. (2005), "Wind effects of parapets on low buildings: part 2. structural loads", *J. Wind Eng. Ind. Aerod.*, **93**(11), 843-855.
- Krajnovic, S. (2011), "Flow around a tall finite cylinder explored by large eddy simulation", *J. Fluid Mech.*, **676**, 294-317.
- Li, Y.Q., Tamura, Y., Yoshida, A., Katsumura, A. and Cho, K. (2006), "Wind loading and its effects on single-layer reticulated cylindrical shells", *J. Wind Eng. Ind. Aerod.*, **94**(12), 949-973.

- Mans, C., Kopp, G.A. and Surry, D. (2005), "Wind effects of parapets on low buildings: part 3. Parapet loads", *J. Wind Eng. Ind. Aerod.*, **93**(11),857-872.
- Okamoto, T. and Yagita, M. (1973), "The experimental investigation on the flow past a circular cylinder of finite length placed normal to the plane surface in a uniform stream", *Bull. JSME*, **16**(95), 805-814.
- Okamoto, S. and Sunabashiri, Y. (1992), "Vortex shedding from a circular cylinder of finite length placed on a ground plane", *J. Fluid.Eng. - TASME*, **114**(4), 512-521.
- Park, C.W. and Lee, S.J. (2002), "Flow structure around a finite circular cylinder embedded in various atmospheric boundary layers", *Fluid Dyn. Res.*, **30**(4), 197-215.
- Park, C.W. and Lee, S.J. (2003), "Flow structure around two finite circular cylinders located in an atmospheric boundary layer: side-by-side arrangement", *J. Fluid. Struct.*, **17**(8), 1043-1058.
- Pattenden, R.J., Turnock, S.R. and Zhang, X. (2005), "Measurements of the flow over a low-aspect-ratio cylinder mounted on a ground plane", *Exp. Fluids*, **39**(1), 10-21.
- Portela, G. and Godoy, L.A. (2005), "Wind pressures and buckling of cylindrical steel tanks with a dome roof", *J. Constr. Steel Res.*, **61**(6), 808-824.
- Purdy, D.M., Maher, P.E. and Frederick, D. (1967), "Model studies of wind loads on flat-top cylinders", *J. Struct. Division - ASCE*, **93**, 379-395.
- Roh, S.C. and Park, S.O. (2003), "Vortical flow over the free end surface of a finite circular cylinder mounted on a flat plate", *Exp. Fluids*, **34**(1), 63-67.
- Shih, W.C.L., Wang, C. and Coles, D. (1993), "Experiments on flow past rough circular cylinders at large Reynolds numbers", *J. Wind Eng. Ind. Aerod.*, **49**(1-3), 351-368.
- Stathopoulos, T. (1982), "Wind pressures on low buildings with parapets", *J. Struct. Division - ASCE*, **108**(12), 2723-2736.
- Stathopoulos, T. and Baskaran, A. (1988), "Wind pressures on flat roofs with parapets", *J. Struct. Eng. - ASCE*, **113**(11), 2166-2180.
- Sumner, D., Heseltine, J.L. and Dansereau, O.J.P. (2004) "Wake structure of a finite circular cylinder of small aspect ratio", *Exp. Fluids*, **37**(5), 720-730.
- Sumner, D. and Heseltine, J.L. (2008), "Tip vortex structure for a circular cylinder with a free end", *J. Wind Eng. Ind. Aerod.*, **96**(6-7), 1185-1196.
- Sun, T.F., Gu, Z.F., He, D.X. and Zhang, L.L. (1992), "Fluctuating pressure on two circular cylinders at high Reynolds numbers", *J. Wind Eng. Ind. Aerod.*, **41-44**, 577-588.
- Uematsu, Y., Yamada, M. and Ishii, K. (1990), "Some effects of free-stream turbulence on the flow past a cantilevered circular cylinder", *J. Wind Eng. Ind. Aerod.*, **33**(1-2), 43-52.
- Uematsu, Y. and Yamada, M. (1994), "Aerodynamic forces on circular cylinders of finite height", *J. Wind Eng. Ind. Aerod.*, **51**(2), 249-265.
- Uematsu, Y. and Yamada, M. (2002). "Wind-induced dynamic response and its load estimation for structural frames of circular flat roofs with long span", *Wind Struct.*, **5**(1), 49-60.
- Uematsu, Y., Watanabe, K., Sasaki, A., Yamada, M. and Hongo, T. (1999), "Wind-induced dynamic response and resultant load estimation of a circular flat roof", *J. Wind Eng. Ind. Aerod.*, **83**(1-3), 251-261.
- Uematsu, Y., Moteki, T. and Hongo, T. (2008), "Model of wind pressure field on circular flat roofs and its application to load estimation", *J. Wind Eng. Ind. Aerod.*, **96**(6-7), 1003-1014.
- West, G.S. and Apelt, C.J. (1982), "The effects of tunnel blockage and aspect ratio on the mean flow past a circular cylinder with Reynolds numbers between 10(4) and 10(5)", *J. Fluid Mech.*, **114**, 361-377.